Parameter and Performance Comparison of Doubly Fed Brushless Machine With Cage and Reluctance Rotors

Fengxiang Wang, Fengge Zhang, and Longya Xu, *Senior Member, IEEE*

***Abstract*—The cage and reluctance rotors are two major types of rotor structures used in the doubly fed brushless machine (DFBM). In order to study comparatively the effects of different rotor structure on the DFBM, a prototype machine has been specially designed and built. The experimental parameter and performance comparisons between the axially laminated anisotropic (ALA) and cage-rotor machines are presented. It is found that the cage-rotor DFBM has better starting and asynchronous characteristics; however, the ALA reluctance-rotor DFBM exhibits better synchronous operation and doubly fed adjustable speed performance.**

***Index Terms*—Cage rotor, comparison, doubly fed brushless machine, performance, reluctance rotor.**

I. Introduction

DOUBLY fed brushless machine (DFBM) adjustable speed system features not only simplicity and reliability of the rotor structure, but also a much smaller power converter in comparison with an adjustable speed system using the conventional singly fed ac motors. In a DFBM, the rotor structure basically determines the magnetic coupling between the two (main and auxiliary) stator windings, which, in turn, determines the machine behavior.

Thus far, individual work has been focused on development of the brushless doubly fed induction machine (BDFIM) with a specially designed cage rotor [1], [2] or of the doubly excited brushless reluctance machine (DEBRM) with an axially laminated rotor [3]–[7]. However, a comparative study for the above two types of DFBMs has yet been examined and compared. It is of the authors' opinion that it is now the time to experimentally investigate performances of the DFBM with different rotor structures of the same size.

In this paper, a prototype machine has been specially designed and built to investigate comparatively the effect of different rotor structures on the parameter and performance of a DFBM. The machine has a common $(6 + 2)$-pole stator and two different rotors of the same size, i.e., the axially laminated anisotropic (ALA) reluctance rotor and the specially designed cage rotor. This paper presents the quantitative comparison of the parameter and performance between the ALA reluctance- and cage-rotor machines based on comparative test results.

Paper IPCSD 02–013, presented at the 2000 Industry Applications Society Annual Meeting, Rome, Italy, October 8–October 12, and approved for publication in the IEEE TRANSACTIONS ON INDUSTRY APPLICATIONS by the Electric Machines Committee. Manuscript submitted for review May 1, 2000 and released for publication May 17, 2002. This paper was supported by the National Natural Science Foundation of China under Research Fund 59577004.

F. Wang and F. Zhang are with the School of Electrical Engineering, Shenyang University of Technology, Shenyang 110023, China.

L. Xu is with the Department of Electrical Engineering, The Ohio State University, Columbus, OH 43210 USA.

Publisher Item Identifier 10.1109/TIA.2002.802917.

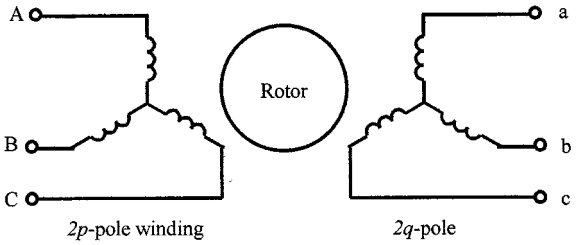

Fig. 1. Schematic diagram of a DFBM.

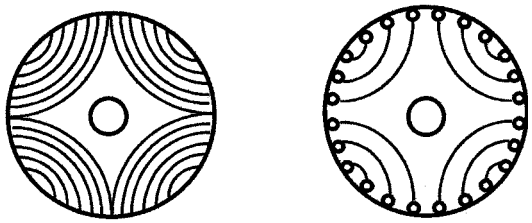

Fig. 2. ALA reluctance and cage rotors.

II. Machine Structure and Operation Mode

The schematic structure diagram of a DFBM is shown in Fig. 1. The two sets of stator windings, i.e., $2p$-pole main and $2q$-pole auxiliary windings, have their own independent three-phase connection. The magnetic mutual coupling between the two sets of stator windings is realized through the specially designed rotor. The two rotor structures for DFBM, i.e., the ALA reluctance and cage rotors, are shown in Fig. 2. If the main stator winding is supplied with ac power and the auxiliary winding is short circuited, the machine will start asynchronously and operate at a asynchronous mode like a $2(p + q)$-pole induction motor. If a dc-excitation current is applied to the auxiliary winding when the rotor speed is near synchronous speed, the rotor will be pulled into synchronization. The DFBM will then be in the synchronous mode like a $2(p + q)$-pole synchronous motor. If the auxiliary winding is supplied with a power converter, the doubly fed adjustable-speed mode of the DFBM can be realized. The rotor speed will be

$$n_r = \frac{60(f_p \pm f_q)}{p + q} \tag{1}$$

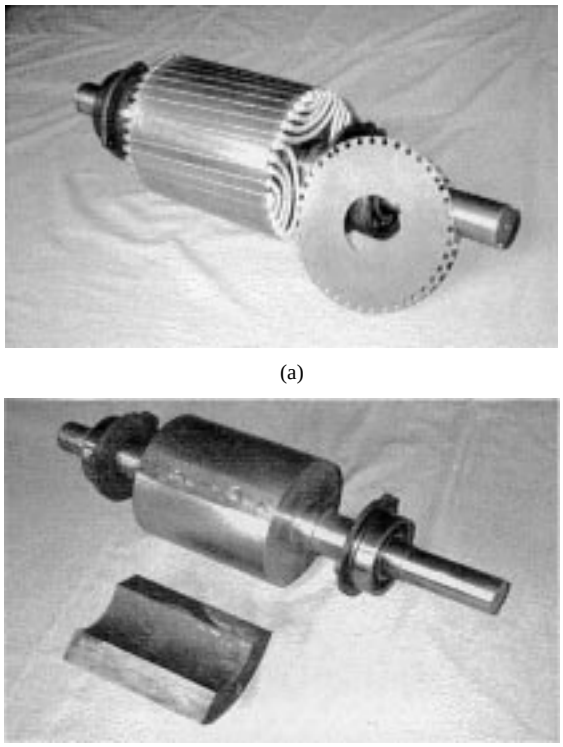

(a)

(b)

Fig. 3. Two structure rotors of prototype DFBM. (a) Cage rotor. (b) ALA reluctance rotor.

where p, f_p and q, f_q are the pole pair number and current frequency of the main and auxiliary windings, respectively. The operation symbol "$\pm$" in the bracket is dependent upon the current phase sequences of the main and auxiliary windings. If the current phase sequence of the auxiliary winding is the same as that of the main winding, the operation symbol "$+$" is taken. Otherwise, the "$-$" should be taken.

In order to evaluate and compare the parameters and performance of a DFBM with different rotor structures, a prototype DFBM has been specially designed and built. The machine has a 36-slot common stator core with two independent three-phase Y-connected windings, one six-pole main, and another two-pole auxiliary windings. Two different structure rotors of the same size, i.e., the ALA reluctance rotor and short-circuited cage rotor, are built and shown in Fig. 3. The main dimensions of the machine are as follows:

outer diameter of stator lamination	260 mm;
inner diameter of stator lamination	170 mm;
effective length of stator stack	195 mm;
length of air gap	0.5 mm;
number of stator slots	36;
number of cage-rotor slots	40.

ALA rotor

number of laminations	5;
ratio of steel to air	2.5 : 1;
saliency ratio	0.63.

The experimental comparison study of the DFBM with two different structure rotors has been carried out with the system diagram shown in Fig. 4. Different operation modes of the DFBM can be realized through the operation mode control device. For the doubly fed adjustable-speed operation mode, a specially designed bidirectional converter is usually needed. However, we have used a commercially available pulsewidth modulation (PWM) inverter, limited to one directional power flow through the inverter, in the experiment. The recorded testing results and analysis for the different operation modes are presented, respectively, in the following sections.

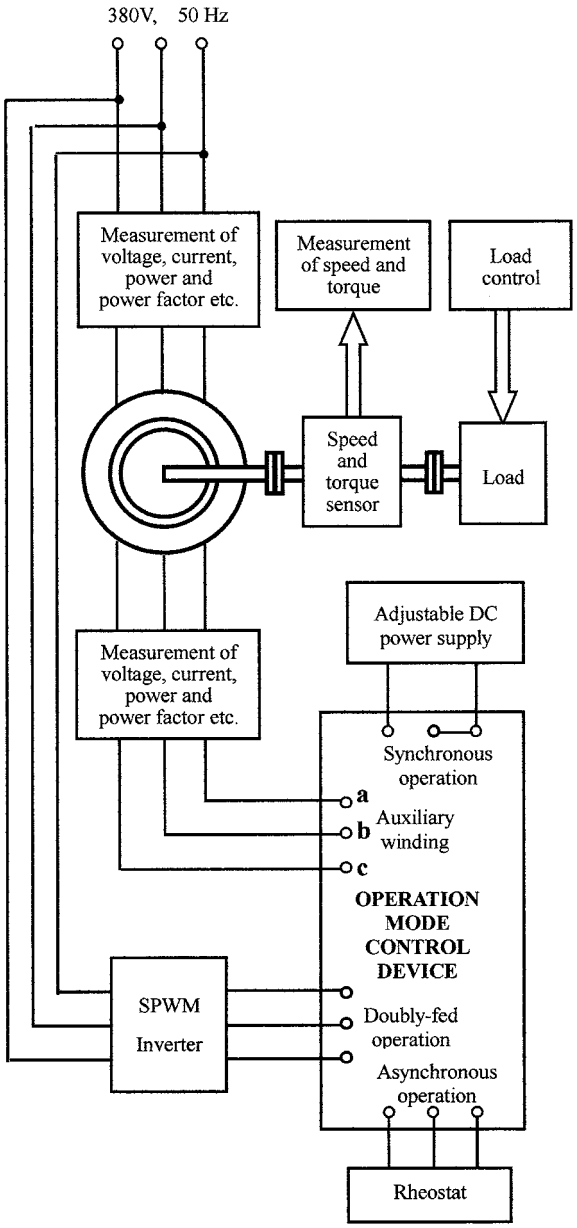

Fig. 4. Experimental system diagram.

III. Self and Mutual Inductance

It can be derived that the steady-state phase-voltage equations of the $2p$- and $2q$-pole stator windings of a DFBM for both the cage and reluctance rotors can be expressed in [7]

$$\boldsymbol{V}_p = R_p\boldsymbol{I}_p + j\omega_p L_p\boldsymbol{I}_p + j\omega_p(L_{pq}\angle\gamma)\left[\boldsymbol{I}_q\angle(-\alpha)\right] \quad (2)$$

$$\boldsymbol{V}_q = R_q\left[\boldsymbol{I}_q\angle(-\alpha)\right] + j\omega_q L_q\boldsymbol{I}_q\angle(-\alpha) + j\omega_q(L_{pq}\angle\gamma)\boldsymbol{I}_p \quad (3)$$

where $\boldsymbol{V}_p$ and V_q, $\boldsymbol{I}_p$ and $\boldsymbol{I}_q$, ω_p, and ω_q, L_p and L_q are the phase voltage, phase current, angular frequency, and self-inductance of the main and auxiliary windings, respectively, L_{pq} is the mutual inductance between the main and auxiliary windings, $(-\alpha)$ is the initial angle of the $2q$-pole magnetomotive force (MMF) with respect to the $2p$-pole MMF, and γ is the angle between the induced phase speed voltage and current.

The electromagnetic torque of DFBM can be expressed as

$$T_e = 3(p+q)L_{pq}I_pI_q\sin\gamma. \tag{4}$$

It is apparent that the winding inductance, particularly the mutual inductance L_{pq}, plays an important role in the electromechanical energy conversion.

The self-inductance and mutual inductance can be determined experimentally in standstill condition of the machine. If the $2q$-pole winding is open circuited and the $2p$-pole winding is supplied with symmetrical three-phase ac power, it is seen from (2) and (3) that the self-inductance L_p and mutual inductance L_{pq} can be determined as follows:

$$L_p = \left[\sqrt{\left(\frac{U_p}{I_p}\right) - (R_p)^2)}\right] \Big/ \omega_p \tag{5}$$

$$L_{pq} = \left(\frac{U_{qo}}{I_p}\right) \Big/ \omega_p \tag{6}$$

where V_p and I_p are the phase voltage and current applied to the $2p$-pole winding, and V_{qo} is the measured open-circuit phase voltage of the $2q$-pole winding. In a similar way, the self-inductance L_q and mutual inductance L_{pq} can be tested.

It should be noted that the self-inductance and mutual inductance are dependent on the rotor position. Therefore, the above test procedure should be carried out for different rotor positions. In order to obtain accurate test results, not only the voltage and current of the windings, but also the rotor position angle should be carefully recorded.

Fig. 5(a) and (b) shows, respectively, the tested self-inductance and mutual-inductance curves versus the rotor position angle of the DFBM with the cage and ALA rotors. For the sake of clarity, only the inductance of one phase (phase $\boldsymbol{A}$ for the six-pole winding and phase $\boldsymbol{a}$ for the two-pole winding) is displayed in Fig. 5(a) and (b).

From a comparison of Fig. 5(a) and (b), it seems that the self-inductance and mutual inductance of the main and auxiliary windings do not have much difference for the two kinds of rotor structure. Therefore, the magnetic coupling ability of the ALA reluctance rotor is similar to that of the cage rotor.

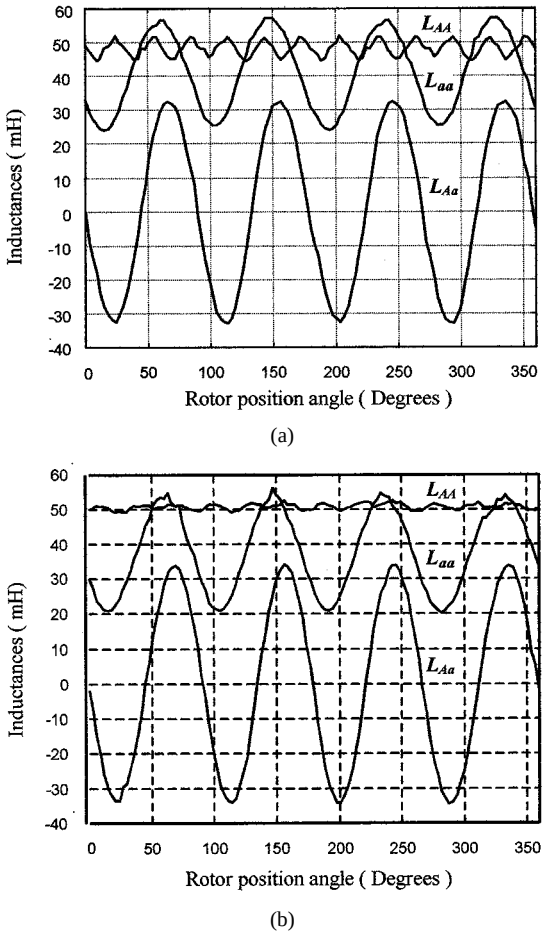

Fig. 5. Tested inductances of a DFBM with different rotors. (a) DFBM with an ALA rotor. (b) DFBM with a cage rotor.

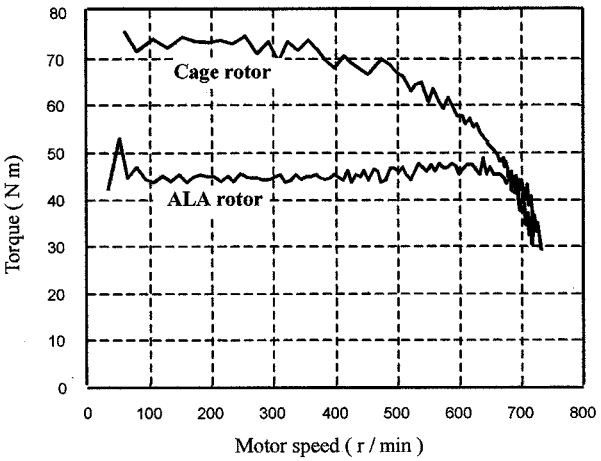

Fig. 6. Comparison of starting characteristic of a DFBM with different rotor structures.

IV. Starting and Asynchronous Operation Characteristics

When the six-pole winding is supplied with three-phase ac power and the two-pole winding is short circuited, the DFBM can be self-started. Fig. 6 shows the comparison of the tested starting characteristics of the DFBM with ALA reluctance and cage rotors under the same condition. The operation conditions are: 1) the two-pole winding terminals are connected together (short circuit); 2) the six-pole winding (Y-connection) is connected to the 380-V (50 Hz) power supply; and 3) the load torque of the machine is 30 Nm.

It can be seen that both the cage rotor and ALA reluctance-rotor DFBM have a good starting characteristic. Compared to the ALA reluctance-rotor machine, however, the cage-rotor machine has much a larger starting torque. In contrast, the ALA rotor machine has a nearly constant torque curve during the entire starting period.

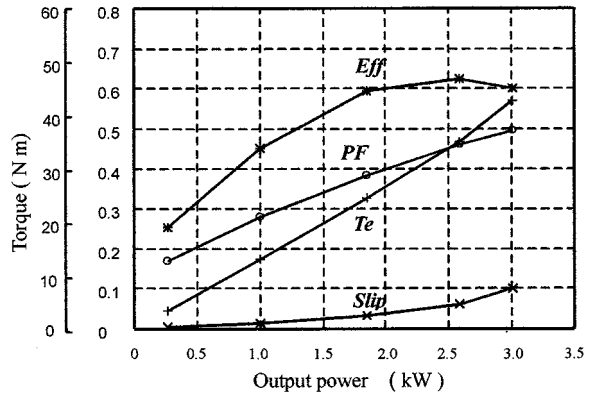

(a)

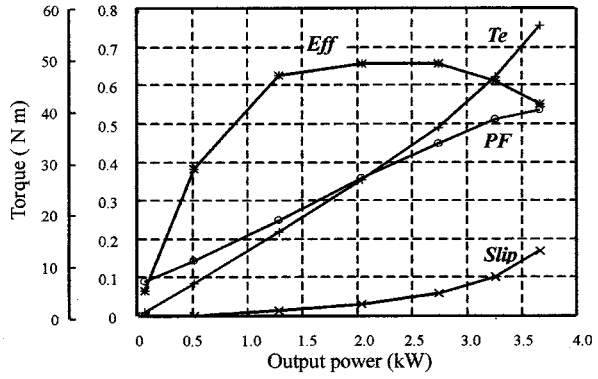

(b)

Fig. 7. Comparison of asynchronous performance of a DFBM with different rotor structures. (a) DEBM with an ALA rotor. (b) DFBM with a cage rotor.

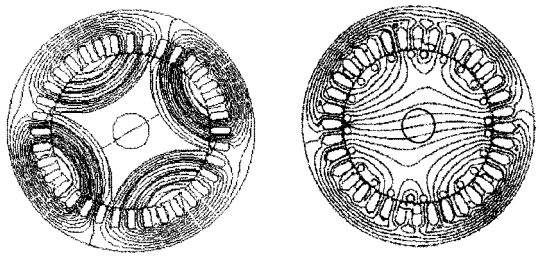

Fig. 8. Comparison of magnetic field in the ALA- and cage-rotor machines.

The (6+2)-pole DFBM, as an equivalent eight-pole induction motor, can be operated at the asynchronous mode. The tested asynchronous performances of the DFBM with two different rotor structures are shown in Fig. 7. The asynchronous characteristics include the efficiency (*Eff*), power factor (*PF*), torque (*Te*), and slip (*Slip*). It can be seen clearly from the comparison of Fig. 7(a) and (b) that the asynchronous performance of the cage-rotor machine is better than that of the ALA reluctance-rotor machine. Why does the cage-rotor machine has larger electromagnetic torque compared to the ALA rotor machine for the asynchronous operation mode? The reason can be explained as follows. Fig. 8 shows the comparison of the magnetic field for the two types of rotor structures. It can be observed that the dominant component in the ALA rotor machine is the eight-pole magnetic field. However, there are other components (six- and two-pole components, etc.), in addition to the eight-pole magnetic field, in the cage-rotor machine.

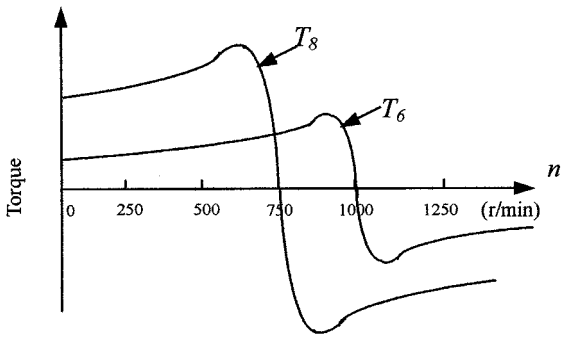

Fig. 9. Schematic diagram of eight- and six-pole asynchronous torque components generated by the cage-rotor DFBM.

However, although the mutual inductances of the main and auxiliary windings do not have much difference for the two kinds of rotor structures, as mentioned above, the MMF of the six- and two-pole windings can be directly coupled with the cage-rotor winding, resulting in correspondent asynchronous torque that affects the total torque of the cage-rotor machine. The effect of the six-pole component on the starting characteristic can be explained schematically, as shown in Fig. 9.

In Fig. 9, there are two torque components. T_8 is the eight-pole asynchronous torque produced by the main and auxiliary winding currents through the mutual inductance coupling. T_6 is the six-pole asynchronous torque produced by the six-pole main winding current and the cage-rotor current like a normal cage-rotor induction machine. As shown in Fig. 9, the synchronous speed of eight- and six-pole torque components are 750 and 1000 r/min, respectively, when the main winding is supplied by a 50-Hz power supply. It is apparent that the six-pole torque component will increase the electromagnetic torque of the cage-rotor DFBM when the machine operates below the synchronous speed. This is the exact reason why the starting and asynchronous operation characteristics of the cage-rotor DFBM are better than that of the ALA rotor DFBM since the latter only has the eight-pole torque component T_8. However, the six-pole torque component does not always play a positive role. Note that whenever the rotor speed going higher beyond 750 r/min, the six-pole torque becomes negative, resulting in a reduced total torque of the cage-rotor DFBM. Compared to the six-pole torque component, the effect of the two-pole component on the performance of the cage-rotor machine is much smaller since its amplitude is much smaller and its synchronous speed is far away from the synchronous speed of the eight-pole component.

As is also seen from Fig. 7, it is difficult to achieve the rated output power of a DFBM. Therefore, it is very unlikely that the asynchronous operation mode is chosen as a normal operational mode for a DFBM.

V. Synchronous Operation Performance

If a dc power supply is supplied to the auxiliary winding, the DFBM will operate in synchronous mode. For dc excitation, the common and practical connection of two phases in parallel and one phase in series is used.

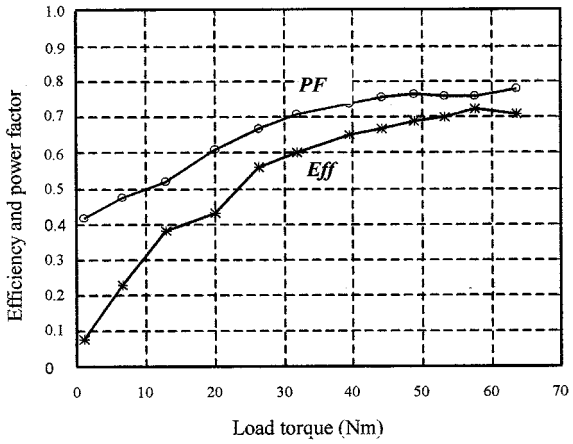

(a)

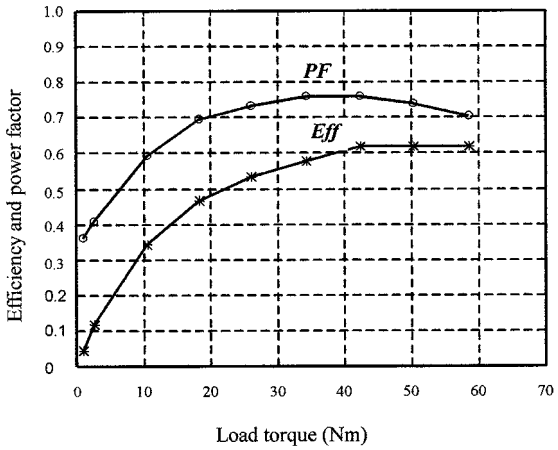

(b)

Fig. 10. Synchronous operation performance of an ALA rotor and cage-rotor DFBM. (a) DFBM with an ALA rotor. (b) DFBM with a cage rotor.

The tested synchronous operation characteristics for the ALA reluctance and cage-rotor DFBM are as shown in Fig. 10(a) and (b), respectively. The rated torque and output power are 50.93 Nm and 4 kW, respectively. It can be seen from the comparison of Fig. 10(a) and (b) that the power factors of the two machines do not have much difference, and the efficiency of the ALA reluctance-rotor machine is higher than that of the cage-rotor machine, which is probably due to the additional cage-rotor losses.

VI. Doubly Fed Adjustable-Speed Operation

One of the most attractive features for a DFBM is that the power converter rating for doubly fed adjustable speed operation can be markedly reduced in comparison with a singly fed variable-speed system. This feature has been proven by the experimental result of the prototype DFBM.

When the six-pole winding is connected to the 380-V 50-Hz ac power supply, the machine speed for both the ALA- and cage-rotor DFBM can be adjusted continuously by changing the frequency of the current applied to the two-pole winding. The tested relationship between the machine speed and current frequency of the two-pole auxiliary winding is shown in Fig. 11. This relationship is exactly the same as expressed in (1). Above

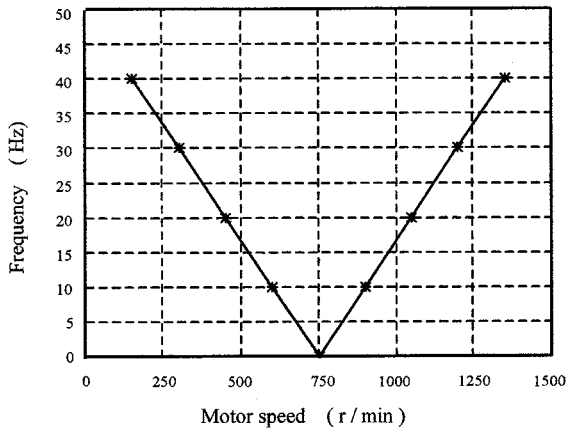

Fig. 11. Relationship between motor speed and frequency of a two-pole winding current.

the synchronous speed (750 r/min), the phase sequence of the auxiliary winding current is the same as that of the main winding current. Below the synchronous speed, the phase sequences of the two winding currents should be opposite.

Referring to Fig. 9, it can be seen that the synchronous speed of the eight-pole torque component will move to the right direction along with the axis of abscissas when the frequency of current supplied to the two-pole auxiliary winding increases. However, the synchronous speed of the six-pole torque component is fixed (1000 r/min) by the current frequency in the six-pole main winding. When the machine operates above 1000 r/min, the negative six-pole torque component will reduce the resultant torque of the cage-rotor DFBM. This analysis has been verified by the experimental result. It is found that the doubly fed operation performance of the cage-rotor DFBM above 1000 r/min is bad and unstable at some speeds. For the sake of clarity, only the tested results of the ALA rotor machine are given here.

The comparative tests clearly show that the doubly fed adjustable speed performance of the ALA rotor machine is much better than that of the cage-rotor machine. The performance of the cage-rotor DFBM is poor above the synchronous speed due to the negative effect of the six-pole torque component. The doubly fed adjustable speed characteristics of the DFBM are also tested for two typical loads, the constant torque load and fan- or pump-type load.

A. Constant Torque Load

Under the constant torque load condition, the tested doubly fed adjustable speed performances of the DFBM with an ALA rotor are as shown in Figs. 12 and 13. The results in Figs. 12(a) and 13 show that the output power of the DFBM is mainly supplied from the six-pole main winding. The power provided by the two-pole auxiliary winding is only a small fraction of the output power, especially within a speed range near the synchronous speed, which is a very attractive feature of the DFBM. Fig. 12(b) shows that the efficiency and power factor can keep a relatively good level over a wide speed range.

B. Fan- or Pump-Type Load

A fan and pump are common loads where the speed needs to be adjusted. The torque of this kind of load is not constant,

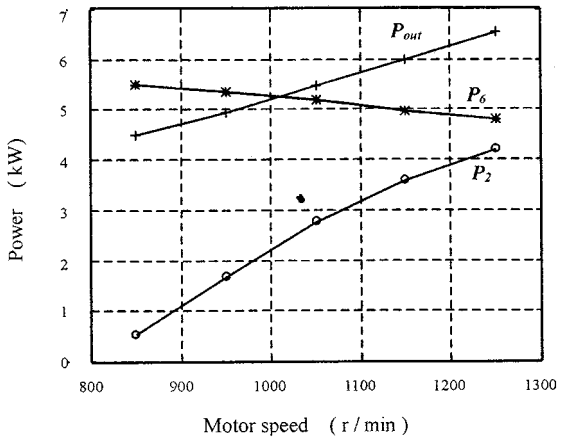

(a)

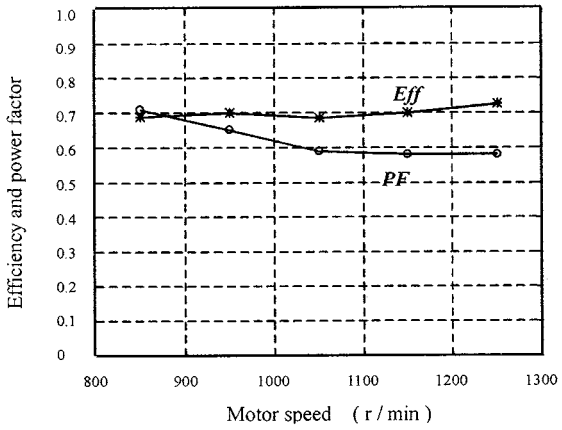

(b)

Fig. 12. Adjustable speed characteristics above synchronous speed (ALA rotor, constant torque load). (a) Relationship between output power, six-, and two-pole winding power. (b) Efficiency and power factor characteristics.

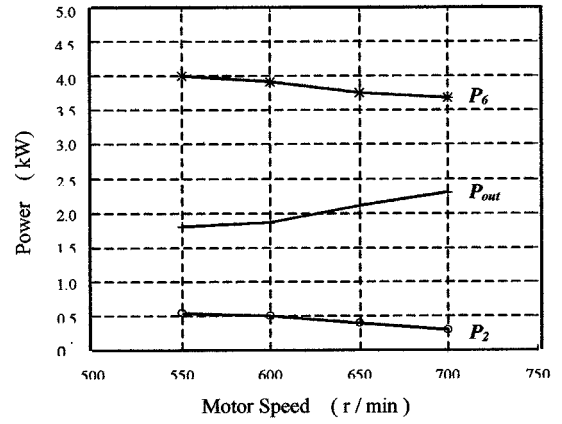

Fig. 13. Adjustable speed characteristics blow synchronous speed (ALA rotor, constant torque load).

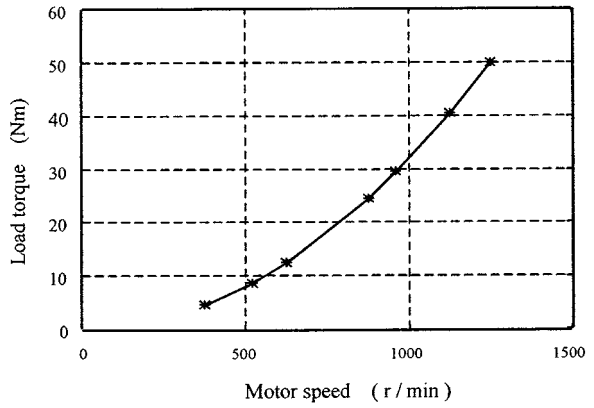

Fig. 14. Characteristic of a fan- and pump-type load.

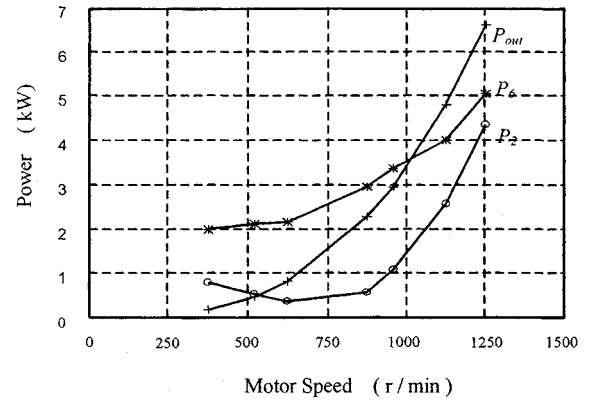

Fig. 15. Power distribution of doubly fed adjustable speed operation for a fan- or pump-type load.

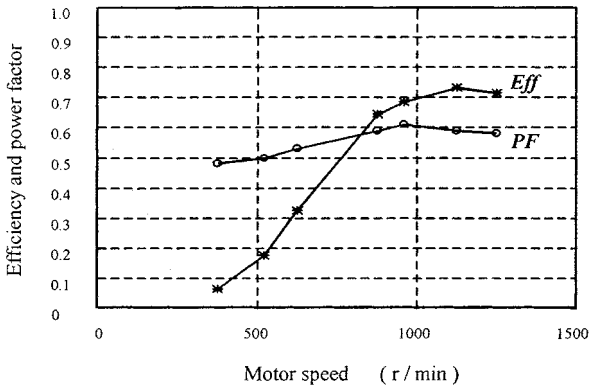

Fig. 16. Efficiency and power factor of doubly fed mode for a fan- or pump-type load.

but proportional to the square of the machine speed. The tested doubly fed adjustable-speed performances of the DFBM with an ALA rotor under the load condition, as shown in Fig. 14, are shown in Figs. 15 and 16. In Fig. 15, the result shows that the two-pole winding power provided by the inverter is small (less than 1 kW) over the speed range from 300 to 900 r/min. Even at the speed of 1000 r/min, the two-pole winding power is only approximately 40% of the machine output power. Fig. 16 shows that the efficiency below the synchronous speed is rather poor. The reason is that the inverter, which is used for the experiment, is not a bidirectional power-flow inverter. Based on the operation principle of the DFBM, the direction of the auxiliary wing power below the synchronous speed should be from the machine to the power supply. However, this cannot be done using a common inverter. The power is injected into the two-pole auxiliary winding in the test for the two cases (above and below the synchronous speed). The output power is provided by the sum of the main and auxiliary winding powers above the synchronous speed. However, the output power is

provided by the difference of the two winding powers below the synchronous speed. That is why the machine efficiency is poor below the synchronous speed. The machine efficiency can be improved by using a bidirectional power-flow inverter.

It should be pointed out that the voltage applied to the two-pole winding can significantly affect the efficiency and power factor of the six-pole winding. In the above doubly fed adjustable-speed operation tests, the voltage applied to the two-pole winding is regulated based on the function of $V_2/f_2 = k$. The efficiency and power factor curves can be different for different voltage applied to the two-pole winding.

VII. Conclusions

From the experimental study of the DFBM with two different kinds of rotor structures, the following conclusions are obtained. For a common stator, the self and mutual inductances of the DFBM with an ALA reluctance rotor or a cage rotor do not have much difference. Thus, the two rotor structures have similar magnetic modulation capability for the two sets of stator windings. However, the six- and two-pole magnetic-field components produced by the direct coupling of the six-pole winding with the cage-rotor winding, and the two-pole winding with the cage-rotor winding are much stronger in the cage-rotor DFBM than that in the ALA rotor DFBM. For the same rotor size, the DFBM with a cage rotor has better starting and asynchronous performance when the auxiliary windings are shorted. However, the DFBM with an ALA reluctance rotor can offer superior performances for the synchronous and doubly fed adjustable-speed operation modes.

References

[1] R. Li, A. Wallace, and R. Spee, "Two-axis model development of cage-rotor brushless doubly-fed machines," *IEEE Trans. Energy Conversion*, vol. 6, pp. 453–460, Sept. 1991.

[2] C. S. Brune, R. Spee, and A. K. Wallace, "Experimental evaluation of a variable-speed, doubly-fed wind-power generation system," *IEEE Trans. Ind. Applicat.*, vol. 30, pp. 648–655, May/June 1994.

[3] C. J. Heyne and A. M. El-Antably, "Reluctance and doubly-excited reluctance motors," Oak Ridge Nat. Lab., Oak Ridge, TN, Final Rep. ORNL/SUB/6 195 013/1, 1984.

[4] F. Liang, L. Xu, and T. A. Lipo, "Analysis of a variable speed doubly AC excited reluctance motor," *Elect. Mach. Power Syst.*, vol. 19, no. 2, pp. 125–138, Mar. 1991.

[5] L. Xu, F. Liang, and T. A. Lipo, "Transient model of a doubly excited reluctance motor," *IEEE Trans. Energy Conversion*, vol. 6, pp. 126–133, Mar. 1991.

[6] L. Xu, Y. Tang, and L. Ye, "Comparison study of rotor structures of doubly-excited brushless reluctance machine by finite element analysis," *IEEE Trans. Energy Conversion*, vol. 9, pp. 165–172, Mar. 1994.

[7] Y. Liao, L. Xu, and L. Zhen, "Design of a doubly fed reluctance motor for adjustable-speed drives," *IEEE Trans. Ind. Applicat.*, vol. 32, pp. 1195–1203, Sept./Oct. 1996.

[8] L. Xu and F. Wang, "Comparative study of magnetic coupling for a doubly-fed brushless machine with reluctance and cage rotors," in *IEEE Ind. Applicat. Soc. Annu. Meeting*, New Orleans, LA, 1997, pp. 326–332.

Fengxiang Wang received the B.E.E. and M.S. degrees from Tsinghua University, Beijing, China, in 1962 and 1966, respectively.

In 1966, he joined the Shenyang University of Technology, Shenyang, China, where he is currently a Professor and the Director of the Electrical Control Technology Institute. From 1981 to 1983, he was a Visiting Scholar with the University of Wisconsin–Madison. From 1992 to 1993, he was a Senior Visiting Scholar with the University of Toronto, Toronto, ON, Canada. From 1996 to 1997, he was a Visiting Professor with the Department of Electrical Engineering, The Ohio State University, Columbus. His major interests are electrical machines and drives, power electronics, and electromagnetics.

Prof. Wang is a member of the China Electrotechnical Society and the Chinese Society for Electrical Engineering. He was the recipient of the 1982 IEEE IAS Paper Prize presented by the Industry Drive Committee.

Fengge Zhang received the B.E.E., M.S., and Ph.D. degrees from the Shenyang University of Technology, Shenyang, China, in 1984, 1990, and 2000, respectively.

Since 1984, he has been with the School of Electrical Engineering, Shenyang University of Technology, where he is currently a Professor. His research interests include electromagnetic theory, modeling, simulation, optimized design, and power converters. He is currently a Visiting Professor with the Fachhochschule Esslingen-Hochschule für Technik, University of Applied Sciences, Esslingen, Germany.

Longya Xu (S'89–M'90–SM'93) received the M.S. and Ph.D. degrees in electrical engineering from the University of Wisconsin–Madison, in 1986 and 1990, respectively.

In 1990, he joined the Department of Electrical Engineering, The Ohio State University, Columbus, where he is currently a Professor. He has served as a Consultant to many industrial companies, including the Raytheon Company, U.S. Wind Power Company, General Motors, Ford, and Unique Mobility Inc. His research and teaching interests include dynamic modeling and optimized design of electrical machines and power converters for variable-speed generating and drive systems, and application of advanced control theory and digital signal processors in controlling motion systems for super-high-speed operation.

Dr. Xu currently serves as the chairman of the Electric Machines Committee of the IEEE Industry Applications Society (IAS) and as an associate editor of the IEEE Transactions on Power Electronics. He was the recipient of the 1990 First Prize Paper Award presented by the IEEE IAS Industrial Drives Committee. He was the recipient of the 1991 Research Initiation Award presented by the National Science Foundation. He was also a recipient of the 1995 and 1999 Lumley Research Awards for his research accomplishments presented by the College of Engineering, The Ohio State University.